10

Carbon Nanotube Systems to Communicate With Enzymes

J. Justin Gooding and Joe G. Shapter

Summary

The efficient transfer of electrons between enzymes and electrodes is important for understanding the intrinsic redox properties as well as for developing protein-based biosensors and bioelectronic devices. One strategy to achieve efficient electron transfer to proteins is to build up the electrode inside the protein so that it is close to the redox-active center of the protein. To achieve this requires exceedingly small electrodes. Carbon nanotubes, which are as small as 1 nm in diameter, have the potential to be such electrodes. This chapter outlines recent research toward this goal via the self-assembly of vertically aligned single-walled carbon nanotubes on electrode surfaces followed by the subsequent attachment of proteins to the free ends of the tubes.

Key Words: Carbon nanotubes; self-assembly; microperoxidase MP-11; glucose oxidase; electrochemistry; enzyme electrodes; alkanethiols; self-assembled monolayers; atomic force microscopy.

1. Introduction

Research into the interaction and electron exchange between redox enzymes and an electrode interface is important for two reasons: first, it is helpful to understand the intrinsic redox properties of proteins ***(1,2)***; and second, direct electron transfer between enzymes and electrodes is the key to the development of mediatorless, also called third-generation, enzyme biosensors. With a mediatorless biosensor, no cosubstrate is required in the recycling of the enzyme back to its active form. This concept of the mediatorless enzyme biosensor is most applicable to the oxidoreductase enzymes where, as shown in **Scheme 1** for glucose oxidase, the enzyme oxidizes glucose and is reduced in the process. The recycling of the enzyme back to its active oxidized form is achieved using either oxygen in nature or another mediating species such as ferrocene (as used in many glucose meters). The ability of the enzyme

From: *Methods in Molecular Biology, vol. 300:*
Protein Nanotechnology, Protocols, Instrumentation, and Applications
Edited by: T. Vo-Dinh © Humana Press Inc., Totowa, NJ

$$GOD_{FAD} + G \underset{k_{-1}}{\overset{k_1}{\rightleftharpoons}} GOD\text{-}G \xrightarrow{k_2} GOD_{FADH_2} + Gluconolactone$$

$$GOD_{FADH_2} + O_2 \xrightarrow{k_3} GOD_{FAD} + H_2O_2$$

Scheme 1. Reaction mechanism for glucose oxidase oxidizing glucose to gluconolactone.

to be oxidized and reduced directly at the electrode would obviate this second reaction, which has implications for reliably sensing in vivo and in other environments where cosubstrate concentration may vary.

The redox centers of most redox-active biological molecules are imbedded deep within the glycoprotein ***(1)***. For example, in the case of glucose oxidase, the closest approach between the exterior of the protein and the redox-active center flavin adenine dinucleotide (FAD) is 13 Å ***(3)***. As a consequence, electrons cannot be efficiently transferred between the enzyme and the electrode and hence, mediators, or redox relays, are required. There are some exceptions, such as the peroxidase enzymes, laccase and "blue" copper protein, and azurin, in which the redox centers are located close to the surface of the protein and, hence, can be interrogated electrochemically. There have been a variety of approaches to improving the communication between the electrode and the enzyme that usually involve modifying either the electrode or the protein to allow a more intimate association between the protein and the electrode.

Pyrolytic graphite edge-plane electrodes ***(4)*** and self-assembled monolayer (SAM)–modified gold electrodes ***(5)*** have most frequently been used to achieve efficient communication to proteins. The edge planes of pyrolytic graphite contain many organic functionalities such as alcohols, phenolics, carboxylic acids, and other carbonyls. These edge planes allow rapid electron transfer while often maintaining the proteins in their functional state. Pyrolytic graphite, however, provides macroscopic surfaces on which many enzyme molecules will bind. Thus, although the communication between enzymes and the electrode is often effective, there is no control over probing individual enzymes or building up bioelectronic systems on the molecular level. However, this may be possible using carbon nanotubes (CNTs) as electrodes with which to communicate with enzymes.

1.1. CNT Electrodes for Communicating With Redox Proteins

CNTs are hollow cylinders consisting of graphene sheets wrapped in a cylinder ***(6)*** with the ends capped or open. In the case of multiwalled CNTs (MWCNTs), the concentric graphite tubules are in the range of 2 to 25 nm in diameter with 0.34 nm between the sheets. With single-walled CNTs (SWCNTs), a single graphene sheet is rolled seamlessly into individual cylinders of typi-

cally 1 to 2 nm with capped ends. All the carbon atoms are sp^2. SWCNTs can be metallic conductors, semiconductors, or small-band gap semiconductors, depending on their diameter and chirality ***(7)***. Closed nanotubes can be opened in oxidizing environments such as nitric acid. Open-ended nanotubes have been shown to have excellent electron transfer properties ***(2,8–10)*** compared with closed nanotubes. The open ends of the CNTs typically contain carboxylate and quinone functionalities in common with edge planes of pyrolytic graphite. Hence, the open ends can be likened to edge planes of pyrolytic graphite, and the walls have similar electron transfer properties to the basal planes of pyrolytic graphite.

Electrodes have been made using either MWCNTs or SWCNTs. In most of the nanotube electrodes thus far presented in the literature, the electrode is prepared by forming a paste with a filler compound and packing it into an electrode body or simply by dispersing the tubes in a solvent, drop coating onto the electrode to leave a bed of nanotubes on an electrode surface. Electrodes made in this way have been shown to have electrocatalytic properties for ferricyanide ***(11)*** and some biologically relevant molecules ***(8,12,13)***. This electrocatalytic performance is well demonstrated in a recent article by Wang et al. ***(14)*** in which the oxidation and reduction of hydrogen peroxide, a product of most oxidase enzyme reactions, was observed at potentials far lower than that observed with other carbon surfaces. The low potential then allowed the detection of glucose with only minor interferences from common interferents such as ascorbic acid, acetomidophen, and uric acid. Nanotube-modified electrodes have been further modified with proteins. Proteins have been adsorbed onto the electrodes ***(15,16)*** or covalently attached to the tubes ***(17)*** to allow communication between the enzyme and the electrode.

Davis et al. ***(15)*** provided the first example of achieving electron transfer to proteins using CNT-modified electrodes, in which an electrode of MWCNTs was first opened in nitric acid and then mixed with nujol, bromoform, mineral oil, or water. Cytochrome-*c* and azurin were adsorbed onto and/or within the tubes with retained activity. The nanotubes' electrodes were shown to have an excellent ability to probe the redox sites of these proteins, which was superior to that observed with edge-plane pyrolytic graphite. Similar results have been obtained by others who have probed redox proteins with their active sites close to the protein surface such as cytochrome-*c* ***(10,18)*** and horseradish peroxidase (HRP) ***(19,20)***. In the case of HRP, the rate constant for electron transfer of 2.48 s^{-1} is significantly faster than that observed for HRP at an SAM-modified gold electrode of 0.29 s^{-1} ***(21)***. Yamamoto et al. ***(20)*** also showed that a CNT electrode modified with HRP could be interfaced with a second enzyme, such as glucose oxidase or lactate oxidase, to give a sensor for glucose or lactate, respectively.

CNT-based electrodes have also been employed in communicating with enzymes that do not normally allow direct communication, namely glucose oxidase ***(2,22)***. In an investigation by Guiseppi-Elie et al. ***(22)***, a bed electrode of activated SWCNTs was prepared and the enzyme was adsorbed onto this electrode. It was suggested that direct electron transfer to glucose oxidase was possible because adsorption onto the activated nanotubes permitted small assemblies of nanotubes to locate within tunneling distance of the FAD prosthetic group of the enzyme. The rate of electron transfer was found to be 1.7 s^{-1}. A very similar rate of 1.6 s^{-1} was reported by Zhao et al. ***(2)***, in which glucose oxidase-modified nanotube electrodes were fabricated in the same way with the exception that MWCNTs were used. Interestingly, the rate of electron transfer was identical to that quoted for glucose oxidase adsorbed onto anodized graphite electrodes ***(23)*** but significantly faster than the 0.026 s^{-1} quoted when the glucose oxidase was covalently attached to SAM-modified gold electrodes ***(24)***.

The direct electron transfer studies of glucose oxidase illustrate the potential advantages of CNT-modified electrodes. However, all these studies employed randomly entangled nanotubes, which give a poorly defined electrode surface and poorly defined protein immobilization. Such surface studies strongly indicate that the electron transfer is occurring predominantly the ends of the tubes ***(2,8–10)***, although it is known from many studies that the proteins are adsorbed along the walls of the tubes as well as the ends ***(15–17,22,25–27)***. Sotiropoulou and Chaniotakis ***(28)***, however, reported some selectivity of adsorption of glucose oxidase to the ends over the walls of MWCNTs.

Aligned nanotube electrodes will provide a more controlled surface on which to immobilize and communicate with redox proteins. Electrodes of single nanotubes ***(29)*** and aligned arrays of nanotubes ***(11,28,30,31)*** have been fabricated. Of these initial studies, only Gao et al. ***(31)*** and Sotiropoulou and Chaniotakis ***(28)*** have modified the aligned nanotube electrodes. Gao et al. ***(31)*** electrochemically deposited conducting polymer sheaths around the nanotubes, and Sotiropoulou and Chaniotakis ***(28)*** adsorbed glucose oxidase onto the tubes. We also modify aligned nanotube electrodes with redox enzymes with a view to providing efficient direct electron transfer between enzymes and electrodes.

1.2. Aligned CNT Electrodes for Achieving Direct Electron Transfer to Enzymes

The fabrication of aligned CNT electrodes used in our research first relies on the shortening of SWCNTs by modifying the procedure of Liu et al. ***(32)*** in which the tubes are oxidized in an acid mixture of concentrated sulfuric and concentrated nitric acid (3:1 ratio) while sonicating. The resultant tubes are reduced to lengths of the order of a few hundred nanometers depending on the cutting times. The ends of the shortened tubes are open and terminated with

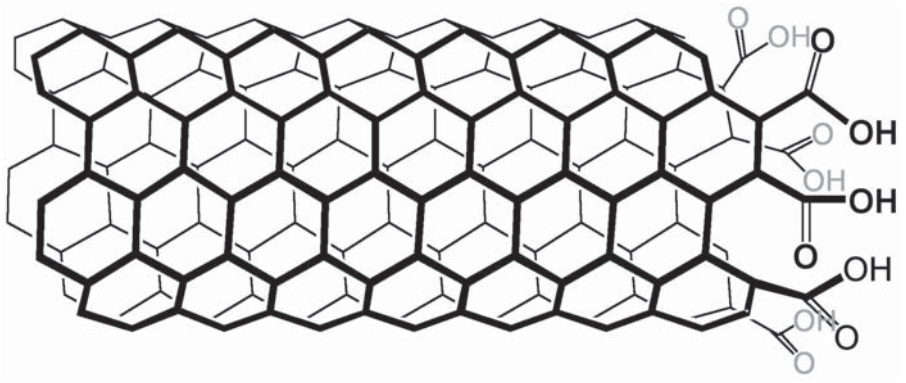

Fig. 1. Representation of shortened SWCNTs with open end showing carboxylic acids formed as consequence of oxidative shortening process.

carboxylic acid moieties (*see* **Fig. 1**). SWCNTs shortened in this way can be self-assembled aligned normal to a surface in a number of ways including by modifying the ends with the alkanethiol cysteamine ($HSCH_2CH_2NH_2$), which is then attached to a gold surface ***(33)***. Other methods include simple assembly of the carboxylic acid-terminated tubes onto a silver surface ***(34)*** or the use of a coordinating ion such as Zn^{2+} ***(35)*** or Fe^{3+} ***(36)*** to anchor the shortened SWCNTs to a surface. We have aligned the shortened SWCNT normal to a gold electrode surface modified with a SAM of cysteamine according to the procedure shown in **Scheme 2**. The nanotubes are covalently linked to the SAM-modified electrode by activating the carboxylic acids with dicyclohexylcarbodiimide (DCC). The aligned CNTs are shown in **Fig. 2**. **Figure 2A** shows what appears to be the SWCNTs standing normally from the gold surface. A cross-section of **Fig. 2A** is shown in **Fig. 2B** in which the height of the tubes attached to the surface appears to be no more than 20 nm. Furthermore, the tubes appear to be in clumps on the surface rather than as individual tubes. If the time the SAM-modified surface is incubated in the tubes is increased, then a greater density of tubes is observed on the surface. Further evidence that these images represent SWCNTs standing from the surface comes from the image in **Fig. 2C**, in which a feature of what appears to be a clump of tubes lying down is visible. The cross section of this image (**Fig. 2D**) shows a large difference in height between this feature and what we believe are the tubes standing normally.

In the activation of the shortened SWCNTs using DCC, both ends of the tubes are activated. Therefore, to the end not attached to the surface, a redox-active species such as an enzyme can be covalently attached (*see* **Scheme 2**). In our work, we have attached ferrocene and the enzymes microperoxidase

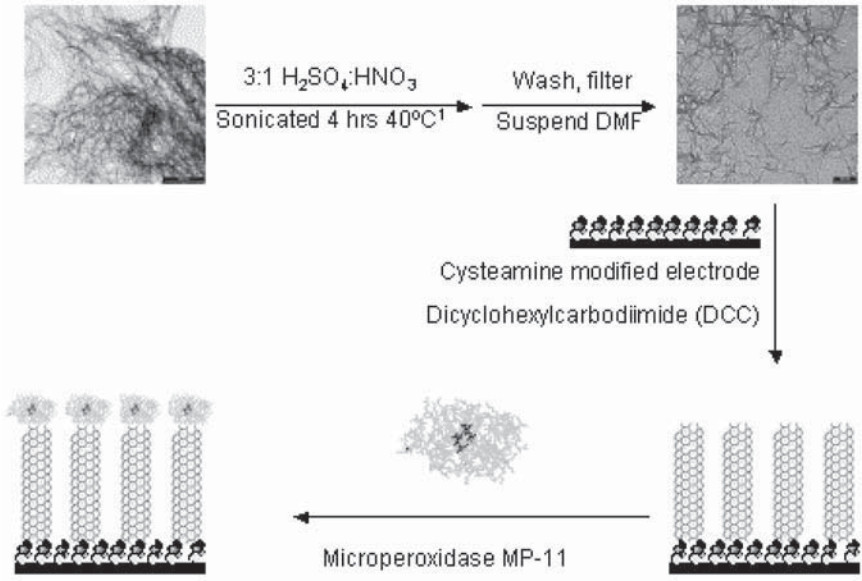

Scheme 2. Steps involved in fabricating aligned shortened SWCNT arrays for direct communication with enzymes such as microperoxidase MP-11 or glucose oxidase.

MP-11 and glucose oxidase. To explore the ability of these aligned SWCNT electrodes to allow direct electron transfer to enzymes, we first investigated the enzyme microperoxidase MP-11 ***(37)*** (**Fig. 3**). MP-11 is a small redox protein, 1.9 kDa, obtained by proteolytic digestion of horse heart cytochrome-*c* ***(38)***, in which the iron protoporphyrin IX is not shielded by a polypeptide. A number of workers ***(38–43)*** have demonstrated that electrons can be efficiently transferred between MP-11 and SAM-modified electrodes.

Attaching MP-11 to the aligned SWCNT-modified gold electrodes and subsequent electrochemical interrogation showed the characteristic peaks for the heme redox-active center of MP-11 with a formal electrode potential of –420 mV vs Ag/AgCl (**Fig. 4**). To verify whether the electrochemistry is owing to MP-11 attached to the ends of the SWCNTs, several control experiments were performed. If a SWCNT bed electrode was prepared by drop coating the shortened SWCNT onto a gold electrode and subsequently adsorbing MP-11 onto the nanotubes, the resultant MP-11-modified electrode showed no redox activity. This control suggests that if the MP-11 is adsorbing onto the walls of the nanotubes, as seems likely from previous work on protein adsorption onto nanotubes ***(15–17,22,25–27)***, the rate of electron transfer through the walls of the tubes is insufficient to give the discernible redox peaks observed in **Fig. 4**.

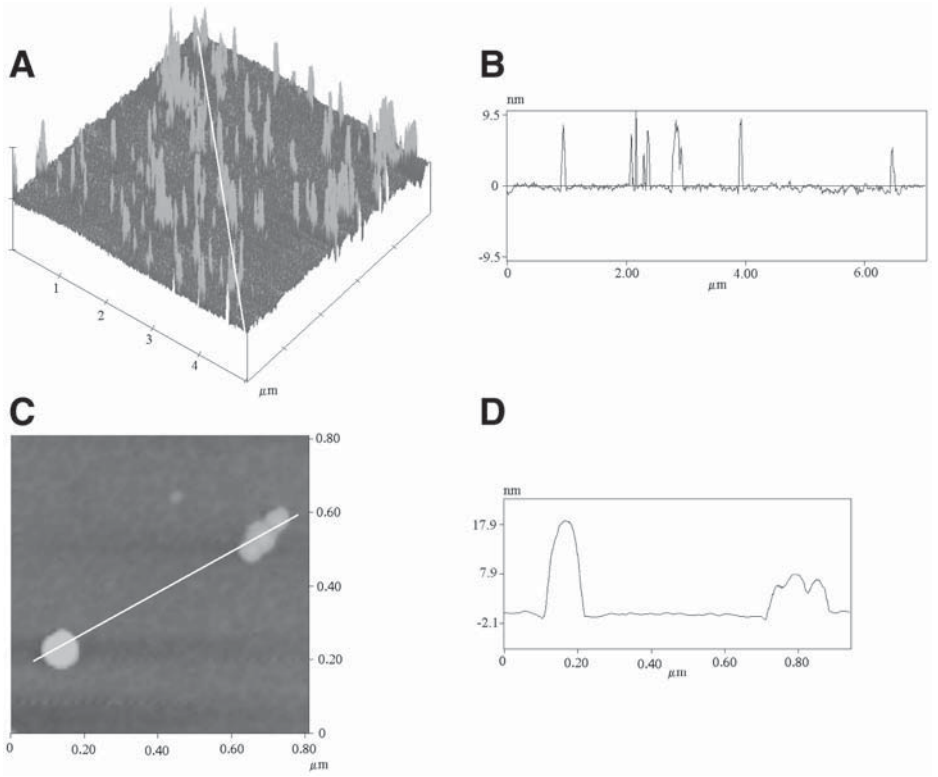

Fig. 2. Atomic force microscopy (AFM) images of shortened SWCNTs aligned onto gold electrode surfaces. **(A)** Tubes cut for 4 h followed by activation with DCC and then incubated with a cysteamine-modified gold electrode for 4 h. The typical heights of the nanotubes are 10 to 20 nm. **(B)** Cross-section of (A) diagonally as shown. **(C)** Top view AFM image showing bundle of aligned nanotubes and another bundle of tubes lying flat on surface. **(D)** Differences in heights between standing tubes and those lying down.

To verify that the electrochemistry was not because of the MP-11 adsorbing onto any cysteamine SAM still accessible between the aligned nanotubes, a cysteamine-modified gold electrode was exposed to MP-11 in an analogous manner to the SWCNT-modified electrodes. In this case, very small MP-11 peaks were observed (**Fig. 4A**), but they were significantly smaller than those observed in **Fig. 4B**. Therefore, we can conclude that the electrochemistry observed in **Fig. 4B** is owing to MP-11 attached to the ends of the SWCNTs with the nanotubes allowing effective communication between the electrode and an enzyme located many nanometers away.

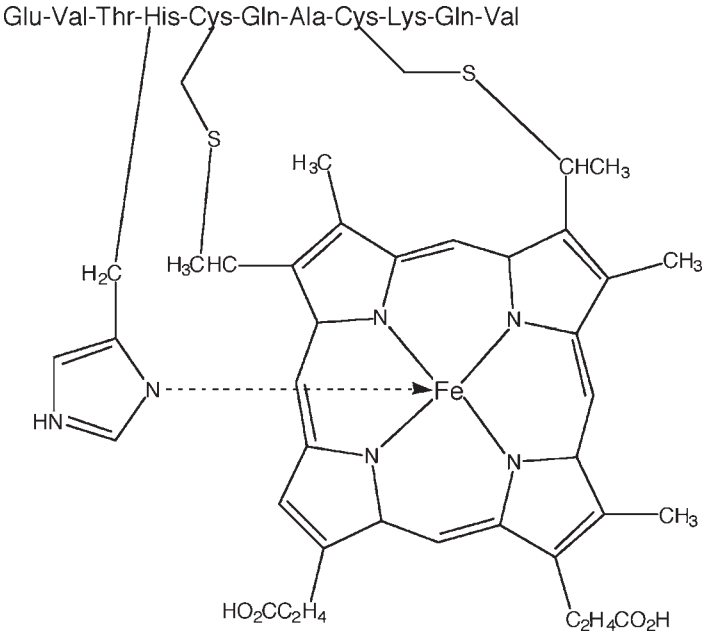

Fig. 3. Microperoxidase MP-11 showing redox-active site and short undecapeptide backbone.

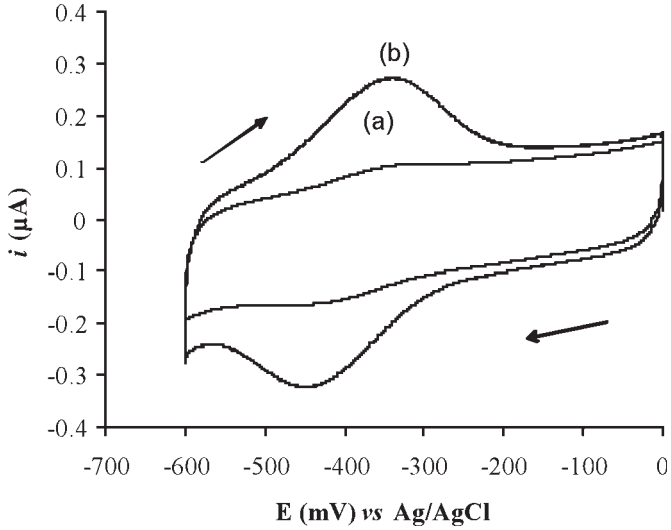

Fig. 4. Cyclic voltammograms of **(A)** Au/cysteamine after immersion into DMF and MP-11 solution and **(B)** Au/cysteamine/SWCNTs/MP-11 in 0.05 *M* phosphate buffer solution (pH 7.0) containing 0.05 KCl under argon gas at scan rate of 100 mV s^{-1} vs Ag/AgCl.

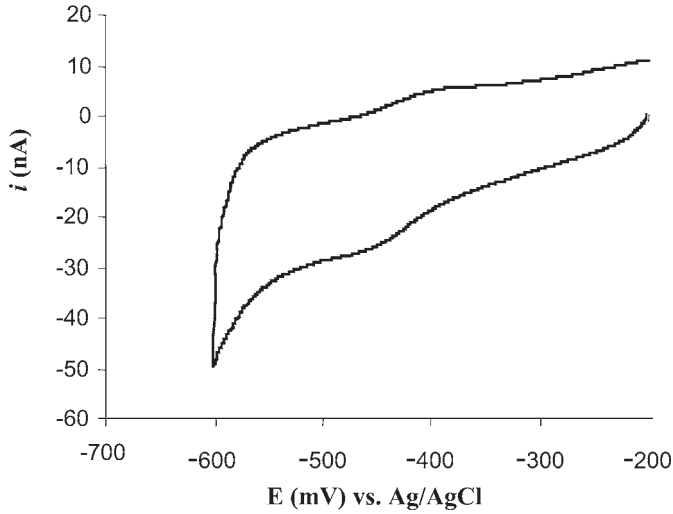

Fig. 5. Cyclic voltammogram of glucose oxidase attached to aligned CNT-modified gold electrode measured in 0.05 *M* phosphate buffer solution (pH 7.0) containing 0.5 *M* KCl under argon gas at scan rate of ×10 mV s^{-1}.

The variation in cyclic voltammograms with scan rate can be used to calculate the rate of electron transfer between the enzyme and the electrode according to the diffusionless model of Laviron ***(44)***. The rate of electron transfer for MP-11 attached to an SWCNT-modified electrode in which the tubes were shortened for 4 h was 2.8 ± 0.9 s^{-1}. This value is only slightly lower than MP-11 attached directly to cysteamine-modified gold electrode (6.1 ± 0.9 s^{-1}) and a 3-mercaptopropionic acid–modified gold electrode (9.4 ± 0.6 s^{-1}). The very similar rate of electron transfer for the MP-11 attached to the nanotubes compared with the equivalent electrode with the nanotubes removed (the cysteamine-modified electrode) demonstrates the efficiency of the nanotubes as molecular wires.

The virtue of SWCNTs in allowing direct electron transfer to redox proteins is reliant on being able to communicate with enzymes in which the redox-active center is imbedded deep within the glycoprotein. The classic example of such a redox protein, as discussed in **Subheading 1.1.**, is glucose oxidase. **Figure 5** shows the electrochemical response of SWCNT-modified electrodes in which glucose oxidase is attached to the ends of the SWCNTs. The small redox peaks, at a formal potential of about –430 mV vs Ag/AgCl, are attributed to the FAD redox center of glucose oxidase. These preliminary experiments indicate that direct electron transfer to glucose oxidase can be achieved. The remainder of this chapter outlines in detail the experimental protocols used to achieve the results presented in this section.

2. Materials

1. Gold working electrode. We used polycrystalline bulk gold electrodes prepared from 1-mm-diameter gold wire (Aldrich, Sydney, Australia) sealed in glass using epoxy (*see* **Note 1**) as described previously ***(45)***. Alternatively, particularly for imaging surfaces, molecularly smooth gold surfaces were prepared by evaporation onto hot mica as described by Mazurkiewicz et al. ***(46)***.
2. Ag/AgCl reference electrode (BAS, Lafayette, IN).
3. Platinum flag counterelectrode (homemade) or, alternatively, from BAS.
4. Electrochemical cell for a three-electrode setup (BAS). Alternatively, we use 20-mL sample tubes with the appropriate number of holes cut into the plastic lid.
5. Polishing cloth and 1-, 0.3-, and 0.05-μ alumina polishing powder (Buehler, Lake Bluff, IL).
6. Ultrasonic cleaner (Unisonics, Sydney, Australia).
7. Potentiostat (BAS 100B).
8. UV-VIS Cary 20 dual beam spectrometer.
9. Scanning Probe Microscopy/Atomic Force Microscopy Digital Instruments Multimode System with a Nanoscope 4 Controller.
10. Phillips CM 200 transmission electron microscope.
11. Carbon nanotubes (Carbon Nanotechnologies, Houston, TX).
12. Solution of concentrated sulfuric acid (98%) and concentrated nitric acid (70%) (3:1 [v/v]).
13. Ethanol (95%).
14. Dimethylformamide (DMF) (Prolabo, Manchester UK).
15. DCC (Aldrich).
16. Teflon membrane, Millipore MF™ membrane filters, type 0.45 μm HA.
17. Hot-plate stirrer.
18. Cysteamine (2-mercaptoethylamine) (Sigma, Sydney, Australia).
19. Microperoxidase MP-11 (Sigma).
20. Phosphate buffer (0.3 *M* NaCl, 5 m*M* phosphate from KH_2PO_4 and K_2HPO_4, pH 7.0).
21. 0.01 *M* HEPES buffer solution, pH 7.5.
22. Eppendorf tubes (500 μL).
23. Argon gas.

3. Methods

3.1. Preparation of Gold Surfaces

1. Polish the gold electrodes to a mirror finish by forming a paste with the alumina powder mixed with Milli-Q water starting with the 1.0-μ paste, then the 0.3-μ alumina, and finishing with the 0.05-μ powder. Polish with each powder for about 5 min by gently drawing figure eights.
2. Place the polished electrodes in a container half filled with Milli-Q water; then place in a sonicator for 10 min.

3. After sonication, fill a clean electrochemical cell with 0.05 *M* sulfuric acid; place the polished gold electrode, a reference electrode, and a counterelectrode; and connect to the potentiostat.
4. Perform a cyclic voltammogram between –300 and 1500 mV with repeated cycling for at least 20 min or until the cyclic voltammogram becomes stable (*see* **Note 2**).

3.2. Cutting of SWCNTs

1. Weigh 2 mg of uncut nanotubes into a sample tube.
2. Add 10 mL of the prepared acid mixture to the nanotubes.
3. Sonicate the sample tubes for the desired time (*see* **Note 3**).
4. Pour the sonicated solution into a beaker and dilute to 500 mL with Milli-Q water.
5. Collect the nanotubes via vacuum filtration with a Buchner funnel using a 0.45-µm pore-size Teflon membrane.
6. Discard the acid and filter 1.5 L of Milli-Q water through the nanotubes to reduce their acidity.
7. Test the pH of the filtrate with a universal indicator to ensure a minimum pH of 5.0 before proceeding. Continue washing with Milli-Q water if the pH <5.0.
8. Immerse the membrane containing the shortened nanotubes in 10 mL of ethanol, sonicate for 15 s (any longer and the membrane will begin to break up), and remove the membrane from the solution with tweezers.
9. Sonicate the ethanol-nanotube solution for 20 min.
10. Pipet 1 mL of the ethanol-nanotube solution into a clean sample tube.
11. Heat the solution to evaporate most of the ethanol, leaving a thin film of ethanol to make the redispersion of the shortened nanotubes easier.
12. Add 10 mL of DMF (0.2 mg mL^{-1}) and shake gently to redisperse the nanotubes. The shortened CNTs are now ready for use.

3.3. Characterization of Lengths of Cut SWCNTs

1. Disperse the original and shortened SWCNTs with different cutting times in ethanol.
2. Place a drop or two of this dispersion onto 3-mm-diameter copper grid.
3. Allow the drop or two to evaporate at room temperature overnight.
4. Insert the sample in the transmission electron microscope and take several pictures.
5. Determine the length of each shortened SWCNT prepared at any cutting time simply by manually measuring the length from the transmission electron microscope images. Use at least 100 individual ropes from the images for the distribution determination (*see* **Notes 3** and **4**).

3.4. Assembly of SWCNTs on Electrode Surfaces

3.4.1. Assembly of Aligned Nanotubes

1. Prepare a 1 m*M* cysteamine solution in 75% aqueous ethanol.
2. Pipet 200 µL of the cysteamine solution into a 500-mL Eppendorf tube.

3. Place a gold electrode (cleaned immediately prior to modification) into the Eppendorf tube so that the gold layer is in the solution.
4. Leave for 5 h for the cysteamine monolayer to self-assemble.
5. Remove the electrode and rinse thoroughly with ethanol.
6. Sonicate the electrode in ethanol for 15 s to remove possible surface contaminants.
7. Pipet 200 µL of the shortened nanotubes dispersed in DMF (0.2 mg mL^{-1}) into an Eppendorf tube and add 0.5 mg of DCC (to give a concentration of approx 2 m*M*).
8. Immerse the cysteamine-coated electrode in the nanotube solution for the desired time (typically 4 h) during which the tubes will covalently attach to the cysteamine coated electrode.
9. Remove the shortened SWCNT-modified electrode and wash in DMF, ethanol, and then phosphate buffer (*see* **Notes 5** and **6**).

3.4.2. Attachment of MP-11

1. Prepare a microperoxidase MP-11 solution at a concentration of 0.5 mg mL^{-1} in HEPES buffer at pH 7.5.
2. Place the shortened SWCNT-modified electrode in the MP-11 solution held at 4°C and incubate overnight.
3. Remove the electrode and rinse in HEPES buffer and then phosphate buffer to remove loosely bound enzyme.

3.5. Atomic Force Microscope Imaging of Aligned SWCNTs

1. Freshly prepare the molecularly smooth gold substrates by template stripping as described previously ***(46)***.
2. Prepare the aligned nanotubes as described in **Subheading 3.4.1.**
3. Use the tapping mode for imaging using commercial Si cantilevers/tips (Olympus) at their fundamental resonance frequencies, which typically varies from 275–320 kHz.
4. Record both height and phase images.
5. Measure the height and length of the SWCNTs using the cross-section analysis using Digital Instruments off-line software (*see* **Note 7**).

4. Notes

1. The cleanliness of the gold surface is all important in determining the quality of the SAM formed on the surface. Hence, even evaporated gold surfaces were cleaned prior to assembly of the modified electrode surface. In the case of polycrystalline gold surfaces, it is important that the epoxy resin used to seal the gold into the glass tube be capable of withstanding the acid conditions used in cleaning. Most epoxy resins will soften in acidic or basic conditions. The epoxy resin that we used was EPON 825 with EPI-CURE 3271 curing agent from Shell Australia, which is resistant to both acidic and basic conditions.
2. The electrochemical cleaning process involves etching away part of the gold surface by oxidizing the surface as the potential is swept anodically (positive). As the potential is swept back negative, the gold oxide that is formed is reduced and a pronounced stripping peak is observed. The additional benefit of the elec-

trochemical cleaning procedure is that the area under this stripping peak can be used to determine the electrochemically accessible area of the gold electrodes. The area of the stripping peak gives the charge passed, and then electrode area can be found using the conversion factor of 480 mC cm^{-2} ***(47)***.

3. The longer the nanotubes are sonicated, the shorter the length distribution but the thicker the bundles the shorten tubes form. The length and width distribution can be determined using either high-resolution transmission electron microscopy or scanning tunneling microscopy in which the tubes are coated onto molecularly smooth gold surfaces fabricated as described previously ***(46)***. Either technique gives the same length distribution, as expected.
4. We have also observed a relationship between the length of the tubes and the mass of the tubes that can be dispersed into various solvents such as DMF. Although we have yet to quantify the length relationship, the amount of tubes that can be dispersed into a given solvent can be monitored via UV-VIS absorption.
5. From this point, they can be used as electrodes or further modified to attach the redox enzymes or other species. The carboxylic acids at both ends of the shortened SWCNTs are activated by the DCC to a carbodiimide that is susceptible to nucleophilic attack from amines. Therefore, to attach species to the other ends of the aligned SWCNTs assembled on the electrode surface simply requires a species with free amines. In our research, we have attached microperoxidase MP-11, glucose oxidase, propylamine, and ferrocene methylamine, synthesized according to the procedure of Kraatz ***(48)***. With the enzymes, amino acids with amine side chains provide the nucleophilic amines for covalent attachments to the SWCNTs. In each case, the attachment procedure is the same with the exception of the solvent to which the molecule to be attached is dissolved. The procedure in **Subheading 3.4.2.** is presented for the attachment of microperoxidase MP-11.
6. With the short chain alkanethiols used in this study, a potential problem is that they are easily oxidized in the presence of light. The result of this oxidation is that the gold-thiolate bond is converted into a gold-sulfinate or gold-sulfonate bond ***(49)***. Both the gold-sulfinate and gold-sulfonate bonds are much less stable than the gold-thiolate bond. Consequently, when performing an electrochemical control with the SAM-modified electrode alone, via cyclic voltammetry, an oxidation peak, owing to the conversion of the sulfinate to the sulfonate, is sometimes observed at approx +0.3 V vs Ag/AgCl. This peak is suppressed on attachment of the tubes. The presence of such a peak also serves as a good guide to the quality of the SAM prior to tube assembly. If the SAM has been prepared such that there is little or no oxidation of the gold-thiolate bond, then no oxidation process will be observed at such low anodic potentials.
7. An important observation from the preliminary experiments is that, although the transmission electron microscope measurements show that length distributions with a mean of approx 100 nm for 4 h cutting, the heights of the tubes in the atomic force microscope (AFM) images are only 10 to 20 nm from the surface. We believe this anomoly is an artifact of the AFM image. Note that the longer the

cysteamine-modified gold surface is incubated in the nanotubes, the higher the density of tubes on the surface. There is also a concomitant increase in mean length of the aligned tubes. These observations provide good evidence that the AFM images are of aligned nanotubes. Further evidence comes from images as shown in **Fig. 2** in which bundles of tubes standing vertically and lying horizontally can be observed.

References

1. Heller, A. (1990) Electrical wiring of redox enzymes. *Acc. Chem. Res.* **23,** 128–134.
2. Zhao, Y. D., Zhang, W. D., Chen, H., and Luo, Q. M. (2002) Direct electron transfer of glucose oxidase molecules adsorbed onto carbon nanotube powder microelectrode. *Anal. Sci.* **18,** 939–941.
3. Hecht, H. J., Schomburg, D., Kalisz, H., and Schmid, R. D. (1993) The 3D structure of glucose oxidase from Aspergillus niger: implications for the use of GOD as a biosensor enzyme. *Biosens. Bioelectronics* **8,** 197–203.
4. Jeuken, L. J. C. and Armstrong, F. A. (2001) Electrochemical origin of hysteresis in the electron-transfer reactions of adsorbed proteins: contrasting behavior of the "blue" copper protein, azurin, adsorbed on pyrolytic graphite and modified gold electrodes. *J. Phys. Chem. B* **105,** 5271–5282.
5. Gooding, J. J. and Hibbert, D. B. (1999) The application of alkanethiol self-assembled monolayers to enzyme electrodes. *TrAC* **18,** 525–533.
6. Bernholc, J., Brenner, D., Nardelli, M. B., Meunier, V., and Roland, C. (2002) Mechanical and electrical properties of nanotubes. *Ann. Rev. Mater. Res.* **32,** 347–375.
7. Niyogi, S., Hamon, M. A., Hu, H., Zhao, B., Bhowmik, P., Sen, R., Itkis, M. E., and Haddon, R. C. (2002) Chemistry of single-walled carbon nanotubes. *Acc. Chem. Res.* **35,** 1105–1113.
8. Britto, P. J., Santhanam, K. S. V., and Ajayan, P. M. (1996) Carbon nanotube electrode for oxidation of dopamine. *Bioelectrochem. Bioenerg.* **41,** 121–125.
9. Luo, H., Shi, Z., Li, N., Gu, Z., and Zhuang, Q. (2001) Investigation of the electrochemical and electrocatalytic behavior of single-wall carbon nanotube film on a glassy carbon electrode. *Anal. Chem.* **73,** 915–920.
10. Wang, J. X., Li, M. X., Shi, Z. J., Li, N. Q., and Gu, Z. N. (2002) Direct electrochemistry of cytochrome c at a glassy carbon electrode modified with single-wall carbon nanotubes. *Anal. Chem.* **74,** 1993–1997.
11. Nugent, J. M., Santhanam, K. S. V., Rubio, A., and Ajayan, P. M. (2001) Fast electron transfer kinetics on multiwalled carbon nanotube microbundle electrodes. *Nano Lett.* **1,** 87–91.
12. Wang, J. X., Li, M. X., Shi, Z. J., Li, N. Q., and Gu, Z. N. (2002) Electrocatalytic oxidation of norepinephrine at a glassy carbon electrode modified with single wall carbon nanotubes. *Electroanalysis* **14,** 225–230.
13. Wang, J. X., Li, M. X., Shi, Z. J., Li, N. Q., and Gu, Z. N. (2002) Investigation of the electrocatalytic behavior of single-wall carbon nanotube films on an Au electrode. *Microchem. J.* **73,** 325–333.

14. Wang, J. X., Musameh, M., and Lin, Y. (2003) Solubilization of carbon nanotubes by nafion toward the preparation of amperometric biosensors. *J. Am. Chem. Soc.* **125,** 2408, 2409.
15 Davis, J. J., Coles, R. J., and Hill, H. A. O. (1997) Protein electrochemistry at carbon nanotube electrodes. *J. Electroanal. Chem.* **440,** 279–282.
16 Balavoine, F., Schultz, P., Richard, C., Mallouh, V., Ebbesen, T. W., and Mioskowski, C. (1999) Helical crystallization of proteins on carbon nanotubes: A first step towards the development of new biosensors. *Angew. Chem. Int. Ed.* **38,** 1912–1915.
17 Huang, W. J., Taylor, S., Fu, K. F., Lin, Y., Zhang, D. H., Hanks, T. W., Rao, A. M., and Sun, Y. P. (2002) Attaching proteins to carbon nanotubes via diimide-activated amidation. *Nano Lett.* **2,** 311–314.
18 Wang, G., Xu, J. J., and Chen, H. Y. (2002) Interfacing cytochrome c to electrodes with a DNA-carbon nanotube composite film. *Electrochem. Commun.* **4,** 506–509.
19 Zhao, Y. D., Zhang, W. D., Chen, H., Luo, Q. M., and Li, S. F. Y. (2002) Direct electrochemistry of horseradish peroxidase at carbon nanotube powder microelectrode. *Sens. Actuators B* **87,** 168–172.
20 Yamamoto, K., Shi, G., Zhou, T. S., Xu, F., Xu, J. M., Kato, T., Jin, J. Y., and Jin, L. (2003) Study of carbon nanotubes—HRP modified electrode and its application for novel on-line biosensors. *Analyst* **128,** 249–254.
21 Gooding, J. J., Erokhin, P., Losic, D., Yang, W. R., Policarpio, V., Liu, J. Q., Ho, F. M., Situmorang, M., Hibbert, D. B., and Shapter, J. G. (2001) Parameters important in fabricating enzyme electrodes using self-assembled monolayers of alkanethiols. *Anal. Sci.* **17,** 3–9.
22 Guiseppi-Elie, A., Lei, C. H., and Baughman, R. H. (2002) Direct electron transfer of glucose oxidase on carbon nanotubes. *Nanotechnology* **13,** 559–564.
23. Chi, Q. J., Zhang, J. D., Dong, S. J., and Wang, E. K. (1994) Direct electrochemistry and surface characterization of glucose oxidase adsorbed on anodized carbon electrodes. *Electrochim. Acta* **39,** 2431–2438.
24. Jiang, L., McNeil, C. J., and Cooper, J. M. (1995) Direct electron transfer reactions of glucose oxidase immobilised at a self-assembled monolayer. *J. Chem. Soc. Chem. Commun.* 1293–1295.
25 Davis, J. J., Green, M. L. H., Hill, H. A. O., Leung, Y. C., Sadler, P. J., Sloan, J., Xavier, A. V., and Tsang, S. C. (1998) The immobilisation of proteins in carbon nanotubes. *Inorg. Chim. Acta* **272,** 261–266.
26 Azamian, B. R., Davis, J. J., Coleman, K. S., Bagshaw, C. B., and Green, M. L. H. (2002) Bioelectrochemical single-walled carbon nanotubes. *J. Am. Chem. Soc.* **124,** 12,664, 12,665.
27 Shim, M., Kam, N. W. S., Chen, R. J., Li, Y. M., and Dai, H. J. (2002) Functionalization of carbon nanotubes for biocompatibility and biomolecular recognition. *Nano Lett.* **2,** 285–288.
28 Sotiropoulou, S. and Chaniotakis, N. A. (2003) Carbon nanotube array-based biosensor. *Anal. Bioanal. Chem.* **375,** 103–105.

29. Campbell, J. K., Sun, L., and Crooks, R. M. (1999) Electrochemistry using single carbon nanotubes. *J. Am. Chem. Soc.* **121,** 3779, 3780.
30. Diao, P., Liu, Z. F., Wu, B., Nan, X., Zhang, J., and Wei, Z. (2002) Chemically assembled single-wall carbon nanotubes and their electrochemistry. *Chem. Phys. Chem.* **3,** 898–901.
31 Gao, M., Huang, S. M., Dai, L., Wallace, G. G., Gao, R. P., and Wang, Z. L. (2000) Aligned coaxial nanowires of carbon nanotubes sheathed with conducting polymers. *Angew. Chem.-Int. Ed.* **39,** 3664–3667.
32 Liu, J., Rinzler, A. G., Dai, H. J., et al. (1998) Fullerene pipes. *Science* **280,** 1253–1256.
33. Liu, Z., Shen, Z., Zhu, T., Hou, S., Ying, L., Shi, Z., and Gu, Z. (2000) Organizing single-walled carbon nanotubes on gold using a wet chemical self-assembling technique. *Langmuir* **16,** 3569–3573.
34. Wu, B., Zhang, J., Wei, Z., Cai, S. M., and Liu, Z. F. (2001) Chemical alignment of oxidatively shortened single-walled carbon nanotubes on silver surface. *J. Phys. Chem. B* **105,** 5075–5078.
35 Yu, X. F., Mu, T., Huang, H. Z., Liu, Z. F., and Wu, N. Z. (2000) The study of the attachment of a single-walled carbon nanotube to a self-assembled monolayer using X-ray photoelectron spectroscopy. *Surf. Sci.* **461,** 199–207.
36 Chattopadhyay, D., Galeska, I., and Papadimitrakopoulos, F. (2001) Metal-assisted organization of shortened carbon nanotubes in monolayer and multilayer forest assemblies. *J. Am. Chem. Soc.* **123,** 9451–9452.
37. Gooding, J. J., Rahmat, W., Liu, J., Yang, W. R., Losic, D., Orbons, S., Mearns, F. J., Shapter, J. G., and Hibbert, D. B. (2003) Protein electrochemistry using aligned carbon nanotube arrays. *J. Am. Chem. Soc.* **215,** 9006–9007.
38 Lotzbeyer, T., Schuhmann, W., Katz, E., Falter, J., and Schmidt, H.-L. (1994) Direct electron transfer between covalently immobilised enzyme microperoxidase MP-11 and a cystamine-modified gold electrode. *J. Electroanal. Chem.* **377,** 291–294.
39 Lotzbeyer, T., Schuhmann, W., and Schmidt, H.-L. (1996) Electron transfer principles in amperometric biosensors: direct electron transfer between enzymes and electrode surfaces. *Sens. Actuators* **B 33,** 50–54.
40. Lotzbeyer, T., Schuhmann, W., and Schmidt, H.-L. (1997) Minizymes: a new strategy for the development of reagentless amperometric biosensors based on direct electron-transfer processes. *Bioelectrochem. Bioenerg.* **42,** 1–6.
41 Narvaez, A., Dominguez, E., Katakis, I., Katz, E., Ranjit, K. T., Ben-Dov, I., and Willner, I. (1997) Microperoxidase-11-mediated reduction of homoproteins: electrocatalyzed reduction of cytochrome c, myoglobin and hemoglobin and electrocatalytic reduction of nitrate in the presence of cytochrome-dependent nitrate reductase. *J. Electroanal. Chem.* **430,** 227–233.
42 Jiang, L., Glidle, A., McNeil, C. J., and Cooper, J. M. (1997) Characterization of electron transfer reactions of microperoxidase assembled at short-chain thiol-monolayers on gold. *Biosens. Bioelectronics* **12,** 1143–1155.
43 Ruzgas, T., Gaigalas, A., and Gorton, L. (1999) Diffusionless electron transfer of microperoxidase-11 on gold electrodes. *J. Electroanal. Chem.* **469,** 123–131.

44 Laviron, E. (1979) General expression of the linear potential sweep voltammogram in the case of diffusionless electrochemical systems. *J. Electroanal. Chem.* **101,** 19–28.
45 Gooding, J. J., Erokhin, P., and Hibbert, D. B. (2000) Parameters important in tuning the response of monolayer enzyme electrodes fabricated using self-assembled monolayers of alkanethiols. *Biosens. Bioelectronics* **15,** 229–239.
46 Mazurkiewicz, J., Mearns, F. J., Losic, D., Rogers, C., Shapter, J. G., and Gooding, J. J. (2002) Cryogenic cleavage used in atomically flat gold surface production. *J. Vac. Sci. Technol. B* **20,** 2265–2270.
47 Hoogvliet, J. C., Dijksma, M., Kamp, B., and van Bennekom, W. P. (2000) Electrochemical pretreatment of polycrystalline gold electrodes to produce a reproducible surface roughness for self assembly: a study in phosphate buffer pH 7.4. *Anal. Chem.* **72,** 2016–2021.
48. Kraatz, H.-B. (1999) Sythesis and electrochemistry of ferrocenemetylamine and its conjugate acid: crystal structure of ferrocenemethylammonium chloride. *J. Organomet. Chem.* **578,** 222–226.
49. Garrell, R. L., Chadwick, J. E., Severance, D. L., McDonald, N. A., and Myles, D. C. (1995) Adsorption of sulfur-containing molecules on gold—the effect of oxidation on monolayer formation and stability characterized by experiments and theory. *J. Am. Chem. Soc.* **117,** 11,563–11,571.